Available online at www.sciencedirect.com

ScienceDirect

Energy Procedia 57 (2014) 2752– 2761

Energy Procedia

2013 ISES Solar World Congress

The design of a solar-driven catalytic reactor for CO_2 conversions

Bo Wei, Reza Fakhrai*, Bahram Saadatfar, Gowtham Mohan, Torsten Fransson

Department of Energy Technology, KTH, Brinellvägen 68, 10044 Stockholm, Sweden

Abstract

The solar energy has been employed to provide the heat for CO_2 conversions for several years except for its use on power generation, since it is one of the most common renewable energy resources and the total amount is enormous; However, the dominant method is to concentrate solar rays directly on reactants, relying on the design and quality of the receivers a lot. The operation and maintenance of the receivers require extra attention due to the delicate structure of the receivers and the potential contamination on the lenses from the chemical reactions. To steer clear of the shortcoming, a solar-driven catalytic reactor has been designed and analyzed in this article. The reactor drives the endothermic reactions with the heat source of hot gases, which are produced in solar receivers upriver, thus the flexible and necessary operations on the catalytic reactor could be peeled off from the solar receiver, and the potential contamination on the optical components in the solar receiver could be avoided. The design processes and details are described, the heat performance is simulated and analyzed, and efficiencies are theoretically calculated in this article. The solar-driven catalytic reactor exhibits the possibility of the practical use of solar energy in CO_2 conversion and recycle.

Selection and/or peer-review under responsibility of ISES.

Keywords: Solar; receiver, chemical conversion; fluidized bed; CFD modeling;

1. Introduction

Nomenclature

A_r	The area of the inlet boundary of the catalytic reactor
A_s	The surface area of all the solid particles

* Corresponding author. Tel.: +46-8-790-7429; fax: +46-8-204161
E-mail address: reza@kth.se.

Selection and/or peer-review under responsibility of ISES.
doi:10.1016/j.egypro.2014.10.307

C	The concentration ratio
C_d	The drag coefficient
C_f	The specific heat of the gas as the fluid phase
C_s	The specific heat of the particles as the solid phase
Ceria	Cerium Oxide, CeO_2
DNI	The direct normal irradiance
d_p	The diameter of the particles
g	The gravity constant
h	The heat transfer coefficient between the gas and the solids
h_b	The height of the bed
Re	The Reynolds number
t	The physical time of the fluidization
q_c	The heat power from the solar concentrator
q_f	The heat power from the solar receiver
q_{sun}	The heat power from the sunshine
Q_f	The heat brought by the gases into the fluidized bed reactor
Q_s	The heat absorbed by the solid particles in the fluidized bed reactor
U_f	The operation velocity of the gas in fluidized bed
U_{mf}	The minimum fluidization velocity in fluidized bed
U_t	The terminal velocity in the fluidized bed
ε	The porosity of the fluidized bed
η_c	The efficiency of the solar concentrator
η_{rec}	The efficiency of the solar receiver
η_r	The efficiency of the fluidized bed reactor
η_{sys}	The efficiency of the whole system
μ	The viscosity
ρ_f	The density of gases as the fluid phase
ρ_p	The density of particles as the solid phase

The demand of fuels has continuously increased during the last half century, but the shortage especially the oil and gas is more and more prominent. Another reason motivating society to explore alternative energy resources is the CO_2 emission which leads to the greenhouse effect. To reduce the threat of CO_2 emission, the alternative renewable and carbon neutral sources are required.

Among the different alternatives, synthetic gas composing of H_2 and CO has been proved to be a promising fuel. H_2 could be produced from water splitting or steam reforming of hydrocarbons with CO as a co-product, and CO could be produced from CO_2 splitting independently. Both of H_2O and CO_2 are easily accessible raw materials. Another important and attractive advantage is that CO_2 is recycled into fuels.

Most of the chemical reactions involved in the production of H_2 and CO are endothermic reactions and require energy as an input source. In fact, the conversion of CO_2 into CO is energy negative, and the process is non-economic; however, with the advancement of in solar energy technology and upcoming new catalysts, the whole method turns to be feasible and economical. Solar energy is mainly used by two ways: solar photovoltaic producing power and solar thermal utilization, which can provide necessary heat for the production of H_2 and CO via chemical conversions.

The method of producing H_2 or CO by direct splitting H_2O and CO_2 requires high temperatures up to 2400K~2800K, which make the direct splitting method not feasible because such high temperatures require special materials for reactors and too much energy input. The production of H_2 and CO via steam reforming of methane, ethane, methanol, ethanol, and other hydrocarbons have been widely tested on metal catalysts supported by ceria, such as Rh, Pt, Pd, Ru, Au, Ni, Zr, Zn, etc., and ceria (CeO_2) itself is also a common catalyst which has an excellent oxygen storage capability. The required temperature for the reforming ranges from 600K to 1000K[1–3]. The disadvantage is that the reforming consumes hydrocarbons as a large cost.

The two-step splitting method has been preferable due to its own advantages. It reduces metal catalysts first, and then feeds H_2O or CO_2 to the reduced metal oxides at lower temperatures. The oxygen in H_2O or CO_2 will be deprived away to oxidize the metal oxides back to the original status, and complete a recycling process. The catalysts mainly refer to ZnO, ZrO_2, CeO_2, FeO, and other metal oxides. The temperature for reducing the metal oxides ranges from 1200K to 2400K depending on the specific mechanism of the reaction, and the temperature for the oxidation of the catalysts ranges from 1000K~1300K [4–8].

Direct solar concentrating receivers are the mainstream reactors for using solar energy to drive the above chemical processes. This type of reactors is designed as different volumetric cavities. The solar rays are reflected and concentrated by concentrators, and then arrive at the receivers, heating up the receivers very fast to a high temperature. The reactants, i.e. the gases and catalyst particles flow through the space in the receivers get heat from the intensive solar irradiation and the radiation from high temperature walls of the receivers. The power of the concentrators could be as high as 20kW and the concentration ratio C could be up to 16000, resulting in a temperature higher than 2200K in the receivers[9,10].

There are some problems on the direct solar concentrating receivers as chemical reactors. The temperature of the walls of the receivers is normally higher than 2200K, due to the fact that a majority of the heat concentrated to the reactors is absorbed by the walls; and the residence time of the particles is short, requiring an intensive heat transfer from the walls by radiation. The high temperatures of the walls require better materials for manufacturing the reactors. The connections and operations on the reactors such as replacing reactants are hard since the receivers are always set on supports above the concentrators. The reactants and products may also contaminate the optical windows through which the concentrated solar rays get into the receivers. The catalyst particles may melt and adhere to the optical components and ruin them. The particles may also accumulate in some areas in the reactors, making the maintenance more troublesome.

Based on the consideration of the problems in direct concentrating reactors, a solar-driven catalytic reactor separated from the solar receiver has been designed, mainly focusing on the two-step method of splitting CO_2 into CO. The reactor is of fluidized bed type, which has been widely used in industries

because of the flexible operation conditions and good gas-solid interactions for chemical reactions. The catalysts in the fluidized bed reactor are heated by the hot gas flow which has gained a high temperature from the solar receiver. The operations and reactions in the reactor do not affect the operations or safety of the solar receiver. The flexibility of the operations is assured and the potential contamination and threat on the receiver are avoided. In the following parts of this article, the design details and processes are described; the performance of the reactor is analyzed by CFD modeling; and the efficiencies of the energy transfer are calculated. N_2 is chosen as the background gas and ceria is chosen to be the catalyst during the design and analysis[11–13].

2. Methodology

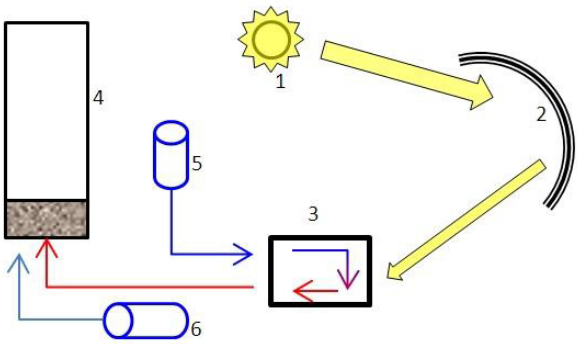

Fig. 1 The diagram sketch of the system

(1). Sun; (2). Concentrator; (3). Receiver; (4). Catalytic reactor; (5). N_2 supply; (6). CO_2 supply

2.1. The system

Fig. 1 shows the system of producing fuel in the catalytic reactor driven by solar energy. The irradiance from the sun is reflected and concentrated by the solar concentrator, and then transferred to the solar receiver. N_2 is heated up in the receiver, and then introduced to the reactor. It heats up ceria particles in the catalytic reactor and brings away the O_2 released by ceria. When ceria is completely reduced into Ce_2O_3, CO_2 is introduced into the reactor to oxidize Ce_2O_3 back into CeO_2, and CO is produced.

2.2. The transfer of the solar energy

The direct normal irradiance (DNI) from the sun is the solar energy arriving at the solar concentrators. It is regarded as 1000W/m^2 in theoretical calculations, and concentrated with a ratio C=1000 and the efficiency of 80%. For a specific receiver, the increase of the operation temperature in the receiver is associated with the drop of the efficiency; however, the efficiency could be enhanced by providing a higher concentration ratio, which means the solar irradiance in a larger area has to be concentrated to the solar receiver. There are already some mature industrial solar thermal facilities which provide gases with a temperature higher than 1200K for power plants[10]. In the design and analysis here, and the temperature of N_2 at the outlet of the receiver is around 1273K. The temperature corresponds with the

efficiency of the receiver η_{rec} of 75%. The heat loss of N_2 along the gas line is neglected, so it is assumed that N_2 enters the reactor with a temperature of 1273K.

2.3. The catalytic reactor

The lab-scale prototype of the catalytic reactor is designed as a vertical cylinder with the diameter of 0.04m and the height of 0.4m to assure an area long enough for the interaction between solid particles and gases. The terminal velocity U_t is a decisive factor dominating the operations of fluidized bed reactors. The velocity is determined by the equation below:

$$U_t = \sqrt{\frac{4(\rho_p - \rho_f) g d_p}{3 C_d \rho_f}} \tag{1}$$

The density of ceria ρ_p is 7220kg/m^3, and the density of nitrogen ρ_f at 1273K is 0.268kg/m^3, with the viscosity of 4.58×10^{-5}Pa·s. Those parameters determine the choice of a uniform diameter of the particles d_p to be 300μm for a better fluidization due to Geldart's theory[14].

The drag coefficient C_d is calculated by:

$$C_d = a + b/\mathrm{Re} + c/\mathrm{Re}^2 \tag{2}$$

In which a, b, c are experiential constants: a=1.22, b=29.17, c=-3.9. The Reynolds number Re at the terminal velocity is calculated by:

$$\mathrm{Re} = d_p U_t \rho_f / \mu \tag{3}$$

The minimum fluidization velocity is calculated by:

$$1823\,\mathrm{Re}_{mf}^{1.07} + 21.27\,\mathrm{Re}_{mf}^{2} = Ar \tag{4}$$

In which $\mathrm{Re_{mf}}$ is the Reynolds number at the minimum fluidization velocity, and Ar is the Archimedes number. The calculations with the above four equations are related to each other, and the values of the parameters are determined with compromise. The equations were solved in the software Ergun 6.2 simultaneously: C_d=4.648, Re=8.371, U_t=4.769m/s, and U_{mf}=0.084m/s.

2.4. The numerical simulation

The numerical simulation was performed with the tool of Ansys/Fluent. A 2D geometry was built and 16000 cells were generated for the grids after meshing. Eulerian multiphase flow model was used to simulate the process of heating the particles with hot gas flow in a fluidized bed. Granular model was used to define the properties and behaviors of the solid phase. Syamlal-Obrien's expression of the granular viscosity and Lun-et-al's expression of the granular bulk viscosity were chosen. The granular temperature was set to be 1×10^{-5}, and the packing limit was set as 0.624 due to the sphere shape of the particles. The restitution coefficient which determined the collisions between the particles was set to be

0.9. The heat transfer coefficient between the two phases was specified by Gunn's expression. The drag coefficient also used Syamlal-Obrein's expression.

In the simulation, the initial temperature of N_2 in the reactor was 1273K based on the assumption of a practical and continuous operation, and the temperature of particles of ceria settled at the bottom of the reactor was 300K. The inlet was set to be a velocity inlet without particles carried by the gas flow, and the outlet was set to be a pressure outlet. The wall of the reactor was assumed to be insulated.

2.5. The heat transfer and efficiencies

The solar energy arriving at the solar concentrator is q_{sun}, and the energy exported from the solar concentrator is q_c. The efficiency of the solar concentrator is:

$$\eta_c = q_c / q_{sun} \tag{5}$$

The efficiency of the solar receiver is

$$\eta_{rec} = q_f / q_c \tag{6}$$

The heat power take by N_2 from the solar receiver is

$$q_f = \rho_f A_r U_f C_f \Delta T_f \tag{7}$$

ΔT_f is the difference between the temperatures of N_2 entering and leaving the solar receiver. The heat absorbed by the particles during the whole heating process is

$$Q_s = \rho_s A_r H_b \cdot (1-\varepsilon) \cdot C_s \Delta T_s \tag{8}$$

The efficiency of the fluidized bed reactor for heating up the catalysts is

$$\eta_r = Q_s / Q_f = Q_s / (q_f \cdot t) \tag{9}$$

The overall efficiency of the system is

$$\eta_{sys} = \eta_c \eta_{rec} \eta_r \tag{10}$$

3. Results

3.1. The flow field during fluidization

The flow fields with different inlet velocities of N_2 were investigated first, to evaluate the fluidization status. The initial height of the bed of ceria was set as 0.04m for a better observation on the fluidization phenomena. The porosity of the bed was 0.376, which means the initial volume fraction of ceria was 0.624, same with the pack limit of the granular phase. After the physical flow time of 1s, the volume

fractions of ceria with different inlet velocities of N_2 were recorded and shown in Fig. 2. The profiles of the volume fractions correspond with the velocities of N_2 of 0.1m/s, 0.2 m/s, 0.4 m/s, 0.7 m/s, and 1 m/s.

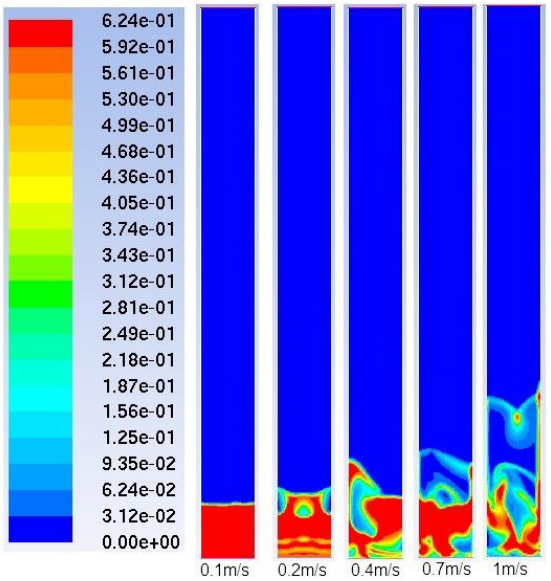

Fig. 2 Volume fractions of particles with different inlet velocities at 1s

When the inlet velocity was 0.1m/s, which was quite close to the minimum fluidization velocity, there was nearly no change in the solid bed, with just a slight expansion that was hard to identify. As the inlet velocity increased to 0.2m/s, the fluidized bed showed clear distinctive layers, and large bubbles appeared. The fluidization became more intensive while the inlet velocity increased to 0.4m/s. The bed was torn up and the particles were fluidized sufficiently. Some particles were blown away from the bed when the velocity was 0.7m/s, and then completely suspending in the space above the solid bed. The phenomena show that 0.4m/s is a proper operation velocity which can fluidize the particles effectively with the least amount of gas. It also proves the experience of fluidized beds that the proper operation velocity of fluidized bed should be 4~5 times of the minimum fluidization velocity.

3.2. The heating performance

The normal heat transfer coefficients in fluidized beds range from 100 to 300W/m^2·K[15]. The total surface area of the ceria particles ranges from 5m^2/g to 100m^2/g depending on the techniques of preparation[16], and a moderate value of 50m^2/g for the surface area is chosen for an estimating calculation here.

$$q_{conv} = hA_s\Delta T \tag{11}$$

With the equation (11), the minimum power that can be transferred from the gas to the solid is estimated as 1.13×10^6W when the initial bed height is 0.04m, even though the temperature difference

between the two phases is just 1K. But for the gas flow with a velocity of 0.4m/s, the maximum power that can be transferred to the particles via equation (6), and it is 159.2W if the gas flow is cooled down from 1273K to 300K.

Assume the particles of ceria are set at the bottom of the reactor, with an initial bed height of 0.04cm, and the power needed to increase the temperature of the particles for 1K in 1s can be calculated with the equation (7). As the result, 104.1W is required for increasing the temperature of the particles by 1K.

It can be known from the estimation that the heating of the particles is not limited by the convection between the two phases, but limited by the heat brought by the gas flow. To decrease the time needed for heating the particles in the investigation, the bed height of the solid particles was set to be 1mm. The temperature distribution of the particles in the reactor at different time is shown in Fig. 3. The temperature profiles correspond with the heating time of 2s, 4s, 6s, 8s, 10s, 12s, 14s, and 20s.

For the particles in the fluidized bed with a bed height of 1mm, they were easily fluidized in the flow field with just a little fraction at the bottom. It can be seen in the figure that the temperature of the particles was quite uniform, because the quantity of the particles was small, and the particles were successfully fluidized in the field. The sufficient fluidization promised the good heat transfer between the gas and the particles by convection. The phenomenon also proves that the heat brought by the gas was competent to heat up the particles in the bed with a bed height of 1mm; otherwise the particles at the bottom would be heated up faster than the particles in the middle area. The facet average temperature of the particles during the heating process was recorded in Fig. 4. It can be seen that the temperature of the particles increased quite fast at the beginning, which means the heat transfer between the particles and the gas was very intensive. As the time passed and the temperature of the particles increased, the paces of the increase became slow, especially when the temperature was higher than 1100K. The time needed for increasing the temperature from 1100K to 1250K was almost the same with the time needed for increasing the temperature from 300K to 1100K. This can be explained because the temperature difference between the particles and the inlet gas was getting less and less, which weakened the heat transfer between them. The heat transfer at the beginning can be hundreds times larger than that in the latter half part of the whole process.

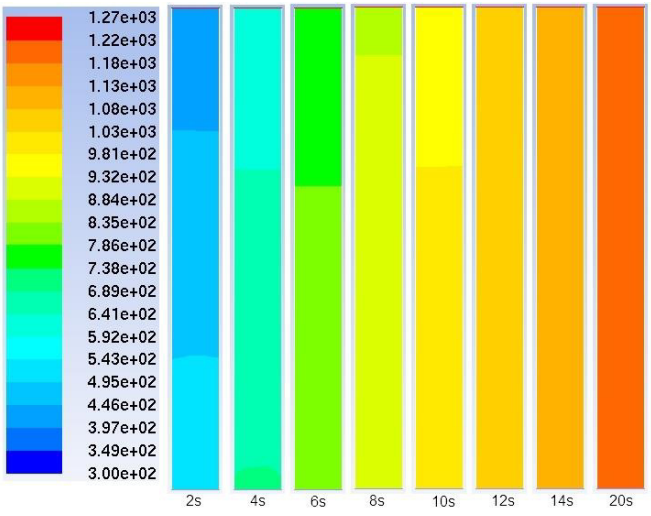

Fig. 3. Temperature distributions of particles at different time

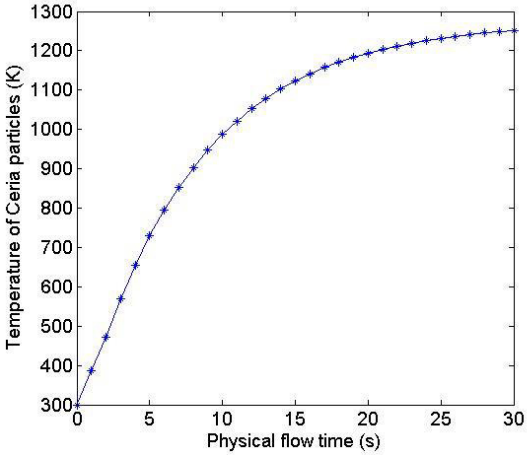

Fig. 4. The temperature of the particles during heating process

3.3. The heat transfer and efficiencies

The particles were heated up for 950K during 30s, and the heat absorbed by the particles can be calculated from the equation (8), with the result Q_s=2472.38J.

The heat brought to the catalytic reactor by the N_2 from the solar receiver during the 30s can be calculated from the equation (7), with the result Q_f=4776J.

Then the efficiency of the catalytic reactor can be calculated from the equation (9), with the result η_r=51.8%.

Since the maximum efficiency of solar concentrator η_c could achieve 80%, and the efficiency of the solar receiver could achieve 75% with a temperature of outlet gas around 1300K by the concentration ratio of 1000, the maximum efficiency of the system can be calculated from the equation (10), with the result η_{sys}≈31.06%.

It can be seen that up to 31.06% of the direct normal irradiance of the solar energy can be transferred to the catalytic reactor for similar two-step conversion reactions by the system designed in the article. The heat power provided to heat up N_2 in the solar receiver is only 159.2W in the investigated case, which is far from the total power that can be provided by the solar receiver. The result means the performance of the reactor can still be largely enhanced by increasing the temperature in the solar receiver with a higher concentration ratio, or increasing the scale of the reactor, to load more catalysts and introduce a larger flow rate of hot gas to use the full capacity of the energy from the solar receiver.

4. Conclusion

A catalytic reactor has been designed and investigated in this article. The reactor is to be used in a solar thermal system to convert CO_2 into CO with two-step splitting method. The solar energy is concentrated and reflected to a solar receiver, and gas flows are heated up in the solar receiver, and then bring the heat to the catalytic reactor to provide heat for the conversions. In the case investigated here, ceria is chosen as the catalyst, and N_2 is chosen to be the background gas. An inlet velocity of 0.2m/s of N_2 can fluidize the particles of ceria with the existence of large bubbles, and a velocity of 0.4m/s of N_2

can fluidize the particles sufficiently. The particles with a bed height of 1mm were set at the bottom of the reactor in advance at a temperature of 300K, and then heated up by N_2 with a temperature of 1273K. It took 15s to heat up the particles to 1100K, and another 15s from 1100K to 1250K. The heat flux at the beginning was much larger than that at the end, due to the decrease of the temperature difference between the solid and the gaseous phases. The efficiency for heating up the particles in the catalytic reactor was 51.8% in this case, which means most of the heat brought by N_2 was transferred to ceria for a temperature increase. A maximum efficiency of 31.06% of the whole system was achieved. The solar radiation was absolutely competent to provide heat for the reactor, since the gas provided to the reactor in the case was just a little fraction of the whole gas flow that heated up by the solar receiver, which meant the solar energy can supply heat to a much larger scale of CO_2 conversions; the operation temperatures of the receiver and the catalytic reactor can also be enhanced largely with a higher concentration ratio. The catalytic reactor shows a competitive ability of heat transfer for CO_2 conversion to produce CO, and also the possibility to separate chemical reactors from solar receivers in solar thermal energy systems; the operation on the reactors could be more flexible and the manufacture and maintenance of the solar receivers could be simplified. This will be the preliminary base for an industrial use.

5. Acknowledgements

The KIC Innoenergy program of the European Union supports the research, and the authors gratefully acknowledge the support.

6. References

[1] Zhang B, Tang X, Li Y, Xu Y, Shen W. Hydrogen production from steam reforming of ethanol and glycerol over ceria-supported metal catalysts. *International Journal of Hydrogen Energy* 2007;32:2367–73.

[2] Corbo P, Migliardini F. Hydrogen production by catalytic partial oxidation of methane and propane on Ni and Pt catalysts. *International Journal of Hydrogen Energy* 2007;32:55–66.

[3] Buck R, Muir J, Hogan R, Skocypec R.. Carbon dioxide reforming of methane in a solar volumetric receiver: the CAESAR project. *Solar Energy Materials* 1991;24:449–63.

[4] Kaneko H, Miura T, Ishihara H, Taku S, Yokoyama T, Nakajima H, et al. Reactive ceramics of CeO_2–MO_x (M=Mn, Fe, Ni, Cu) for H_2 generation by two-step water splitting using concentrated solar thermal energy. *Energy* 2007;32:656–63.

[5] Abanades S, Flamant G. Thermochemical hydrogen production from a two-step solar-driven water-splitting cycle based on cerium oxides. *Solar Energy* 2006;80:1611–23.

[6] Loutzenhiser PG, Elena Gálvez M, Hischier I, Graf A, Steinfeld A. CO_2 splitting in an aerosol flow reactor via the two-step Zn/ZnO solar thermochemical cycle. *Chemical Engineering Science* 2010;65:1855–64.

[7] Stamatiou a., Loutzenhiser PG, Steinfeld A. Solar Syngas Production via H_2O/CO_2 -Splitting Thermochemical Cycles with Zn/ZnO and FeO/Fe_3O_4 Redox Reactions. *Chemistry of Materials* 2010;22:851–9.

[8] Abanades S, Villafan-vidales I. CO_2 valorisation based on Fe_3O_4/FeO thermochemical redox reactions using concentrated solar energy. *International Journal of Energy Research* 2013;37:598–608.

[9] Adinberg R, Epstein M. Experimental study of solar reactors for carboreduction of zinc oxide. *Energy* 2004;29:757–69.

[10] Ávila-Marín AL. Volumetric receivers in solar thermal power plants with central receiver system technology: a review. *Solar Energy* 2011;85:891–910.

[11] Sharma S. Evidence for Oxidation of Ceria by CO_2. *Journal of Catalysis* 2000;190:199–204.

[12] Chueh WC, Falter C, Abbott M, Scipio D, Furler P, Haile SM, et al. High-flux solar-driven thermochemical dissociation of CO_2 and H_2O using nonstoichiometric ceria. *Science* (New York, NY) 2010;330:1797–801.

[13] Chueh WC, Haile SM. A thermochemical study of ceria: exploiting an old material for new modes of energy conversion and CO_2 mitigation. *Philosophical Transactions Series A, Mathematical, Physical, and Engineering Sciences* 2010;368:3269–94.

[14] Geldart D. Types of Gas Fluidization 1973;7:285–92.

[15] Pisters K, Prakash A. Investigations of axial and radial variations of heat transfer coefficient in bubbling fluidized bed with fast response probe. *Powder Technology* 2011;207:224–31.

[16] Laosiripojana N, Assabumrungrat S. Catalytic dry reforming of methane over high surface area ceria. *Applied Catalysis B: Environmental* 2005;60:107–16.